Computational X-ray Imaging using Document Scanners

A. Kadambi[1,*], **A. Cramer**[1,3,*], **R. Lanza**[1], **R. Raskar**[1], **R. Gupta**[2,3]

[1] *Massachusetts Institute of Technology, Cambridge MA 02139*
[2] *Massachusetts General Hospital, Boston MA 02114*
[3] *Harvard Medical School, Boston MA 02115*

e-mail address: achoo@mit.edu

Abstract: We propose a computational imaging approach enabling document scanners to be used as frugal, high-resolution X-ray imagers. We modify the document scanner optics for X-ray sensitivity and design a post-processing algorithm to denoise images.

OCIS codes: 110.0110, 110.1758

1. Introduction

Digital radiography has become the *de facto* standard for X-ray imaging in the developed world. Unfortunately, its advantages — which include ease of image acquisition, visualization, processing, archiving and potential for teleradiology — have not come to large parts of the developing world due to cost and complexity, the primary driver of which is the digital X-ray detector. With that motivation, this paper takes the first steps to turn an ordinary document scanner into a digital X-ray detector using computational imaging.

Specifically, we use a Canon® LIDE 220 document scanner to make X-ray images of a cadaver hand and an X-ray resolution chart. The document scanner is ill-posed to handle low-photon regimes, as would occur when using a scintillation screen. Therefore, both structured and unstructured artifacts are observed in the captured images. These artifacts stem from sources including hardware noise, striped noise from the scanning process, dead pixels, and photon noise from the X-ray beam. We model and mitigate noise using an approach inspired by variational methods [1, 2].

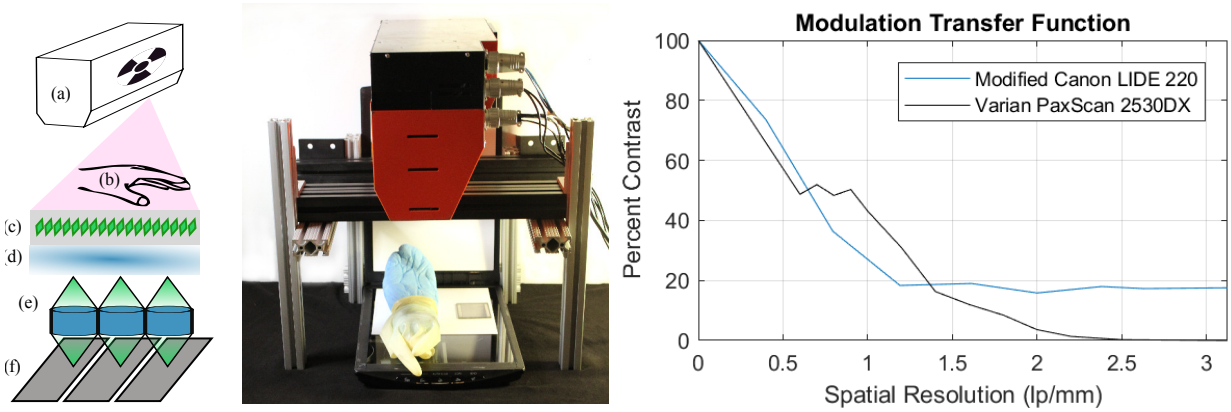

Fig. 1. Optical schematic shown on the left, with (a-f) being X-ray source, imaged object, scintillator, lead-doped glass, GRIN lens, and CMOS. (middle) photo of setup; (right) MTF curves.

2. Optical Configuration

This section describes the hardware modifications made to a Canon® LIDE 220 document scanner. A schematic of our imaging layout and a photograph of our prototype is shown in Figure 1. To enable sensitivity to X-ray radiation, a scintillation screen is placed in front of the scan head to convert X-rays to visible light. The specific scintillation screen we use is made of gadolinium oxysulfide ($Gd_2O_2S:Tb$, peak emission at 550 nm, peak excitation energy at

* These authors contributed equally to the work.

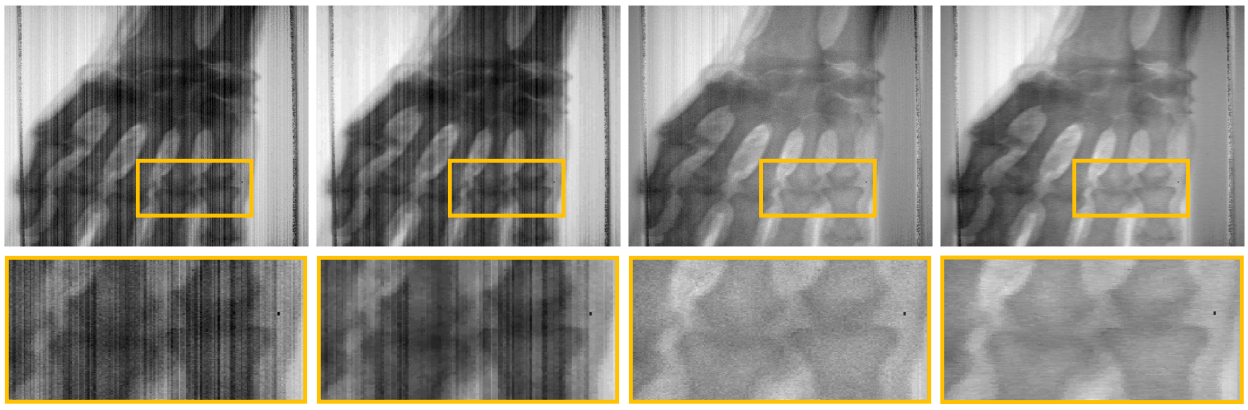

(a) Input: Data Avg from Scanner (b) Best TV denoising (c) Destriping Only (d) Joint Optimization [**Proposed**]

Fig. 2. X-ray image of a cadaver hand using a Canon® LIDE 220 document scanner. The proposed approach is (d). Inset image: proximal inter-phalangeal joint.

110 keV). The object to be imaged is placed on the scintillator and irradiated with X-rays from a Hamamatsu X-ray source (model L9631). Alternate approaches could use a DSLR camera instead of a flatbed scanner [3].

3. Computational Scheme

A document scanner comprises of a 1-D sensor of N pixels, which is moved to M positions. Let $\mathbf{y_m} \in \mathbb{R}^N$ denote the 1-D linescan from the m-th scan head position. The scanner concatenates multiple linescans together to transmit a 2-D image $\mathbf{Y} \in \mathbb{R}^{M\times N}$ to the computer, where $\mathbf{Y} = [\mathbf{y}_1, \ldots, \mathbf{y}_M]$. Since the scintillating screen emits dim light, the measurement $\mathbf{Y}$ results from either a long-exposure scan or an average of multiple scans (described in Section 2). Let $\mathbf{X} \in \mathbb{R}^{M\times N}$ denote the ground truth image, which we aim to recover. We assume an additive noise model, such that

$$\mathbf{Y} = \mathbf{X} + \mathbf{S} + \mathbf{G}, \tag{1}$$

where $\mathbf{S}$ is structured noise and $\mathbf{G}$ is zero-mean Gaussian noise. The structured noise primarily comprises of: (1) stripes due to the push-broom nature of image acquisition and (3) dead lines. Taken together, a joint optimization is written as:

$$\underset{\mathbf{X},\mathbf{S}}{\operatorname{argmin}} \quad \mathscr{C}_{\mathbf{X},\mathbf{S}}(\mathbf{Y}) + \tau\|\nabla_y \mathbf{S}\|_1 + \lambda\|\nabla_x \mathbf{X}\|_1 + \lambda\|\nabla_y \mathbf{X}\|_1$$

where $\mathscr{C}_{\mathbf{X},\mathbf{S}}(\mathbf{Y}) = \|\mathbf{Y} - \mathbf{X} - \mathbf{S}\|_F^2$ denotes the convex functional for the fidelity term and $\|\cdot\|_F$ denotes the Frobenius norm. We defer solution of this optimization program to the full paper.

4. Results

A human cadaver hand was scanned using the modified Canon® LIDE 220, as per the optical description in Section 2. Comparisons were performed with naive averaging (Figure 2a), and a variety of denoising methods. The proposed method is shown in Figure 2d. To quantify spatial resolution, we used a resolution chart benchmark test and a *de facto* X-ray flat panel detector as a control (Figure 1). plots the modulation transfer function of both systems, where it is observed that the flatbed scanner retains 30 percent contrast out to 3.25 lp/mm. This paper is only a first attempt to demonstrate the potential of using consumer document scanners as a method to obtain X-ray images.

References

1. L. I. Rudin, S. Osher, and E. Fatemi, "Nonlinear total variation based noise removal algorithms," Physica D: Nonlinear Phenomena **60**, 259–268 (1992).
2. T. Goldstein and S. Osher, "The split bregman method for l1-regularized problems," SIAM journal on imaging sciences **2**, 323–343 (2009).
3. H. Fan, H. L. Durko, S. K. Moore, J. Moore, B. W. Miller, L. R. Furenlid, S. Pradhan, and H. H. Barrett, "Dr with a dslr: digital radiography with a digital single-lens reflex camera," in "Proceedings of SPIE–the International Society for Optical Engineering," , vol. 7622 (NIH Public Access, 2010), vol. 7622, p. 76225E.